Magnetic Excitations in Strongly Correlated Electrons
J. Phys. Soc. Jpn. **69** (2000) Suppl. B. pp. 65–71

New Two-Dimensional Spin Gap Material $SrCu_2(BO_3)_2$

Hiroshi KAGEYAMA

Institute for Solid State Physics, University of Tokyo
5-1-5 Kashiwanoha, Kashiwa, Chiba 277-8581

(Received December 20, 1999)

I review the magnetic properties of $SrCu_2(BO_3)_2$ from an experimental viewpoint. It is concluded that this material can be regarded as a highly frustrated two-dimensional spin system, realizing the Shastry-Sutherland model with an exact dimer ground state. The spin-gap size, the intra- and interdimer exchange constants were determined to be, respectively, Δ=34 K, J=110 K and J'=75 K. Furthermore, nearly flat band structures of the triplets excitations as well as quantized magnetization plateaux are characterized by a localized nature of the triplets.

KEYWORDS: $SrCu_2(BO_3)_2$, spin gap, orthogonal dimer lattice, Shastry-Sutherland model, exact dimer ground state, magnetization plateaux, spin frustration

§1. Introduction

There has been a continuous progress in the study on the spin gap phenomena that appear in low-dimensional quantum spin systems, in which the ground state is nonmagnetic and there is a finite energy gap in the spin excitation spectrum. In addition, pseudo spin gap behavior observed in High-T_c superconductors accelerated the interest in this field. Now, it is widely accepted that whether a system achieves the spin gapped or gapless ground state crucially depends on the geometry of the spin arrangement, the magnitude of the spin, and appropriate values of exchange constants. Experimentally, many compounds with the spin-singlet ground state have been discovered such as $CuGeO_3$ (S=1/2 quasi-one-dimensional (1D) chain, i.e., spin-Peierls system),[1] Y_2BaNiO_5 (S=1 1D chain, i.e., Haldane system),[2] $SrCu_2O_3$ (S=1/2 intermediate dimensional two-leg ladder)[3] and CaV_4O_9 (S=1/2 2D plaquette system).[4]

Recently, an inorganic layered compound $SrCu_2(BO_3)_2$, which has a novel magnetic network, an S=1/2 2D orthogonal dimer lattice, has been added to the list of the spin gap family.[5] This compound is closely related to the High-T_c superconductors because of (1) the common structures characterized by 2D network of spin-1/2, (2) the (pseudo) spin gap behavior, and (3) an Néel ordered state being closely located in each phase diagram. The most attracting feature in $SrCu_2(BO_3)_2$ is that *the ground state can be solvable exactly*, which was theoretically shown nearly twenty years ago.[6]

The exactness of the ground state allows theoreticians to investigate the magnetic properties of this system in more sufficient depth. It is shown, for example, the triplet excitation is possible only from the sixth order in the perturbation, which means that *the excited triplet is extremely localized*.[7] This localized nature has been experimentally confirmed by the quantized plateaux in the magnetization curve[5] and the almost flat band structures in the spin excitation spectra.[8]

This article is organized as follows: In § 2, the structural features of $SrCu_2(BO_3)_2$ will be mentioned. After quoting the sample preparation in § 3, the spin gap behavior will be discussed in § 4 from the analysis of, e.g., magnetic susceptibility and specific heat measurements, showing how *clean and simple* the ground state is. Section 5 will be devoted to the excitation phenomena based mainly on the results of magnetization curve and inelastic neutron scattering.

§2. Crystal Structure

$SrCu_2(BO_3)_2$ has a tetragonal unit cell with the cell constants of a=8.995 Å and c=6.649 Å at room temperatures.[9] The crystal structure viewed along the c axis is depicted in Fig. 1(a), which is characterized by the layers of interconnected rectangular planar CuO_4 and triangular planar BO_3 groups. The $CuBO_3$ layers extend parallel to the c axis and are structurally separated from each other by planes composed of nonmagnetic Sr^{2+} ions. All Cu^{2+} ions that carry spin-1/2 are located at crystallographically equivalent sites. A unique 2D magnetic linkage of the Cu^{2+} spins is formed as illustrated in the left-hand of Fig. 1(b). The nearest-neighbor Cu ions with the distance of 2.905 Å share edge to form dimeric units, which are connected orthogonally through B^{3+} ions, providing pathways for interdimer interaction (the interdimer

distance is 5.132 Å). Strictly speaking, the dimers in each plane are not in the same plane: the plane of horizontal dimers is slightly shifted from the plane of vertical dimers.

Because of the good two-dimensionality of the crystal structure, the magnetic properties should be described by the Heisenberg model with the intradimer and interdimer exchange interactions symbolized by J and J', respectively. The lattice of $SrCu_2(BO_3)_2$ is compared with that studied theoretically by Shastry and Sutherland nearly twenty years ago (see the right-hand of Fig. 1(b)).[6] By lengthening the dimer bonds of the former lattice, one can change the real lattice to the imaginary one, indicating that they are topologically equivalent. An important point of this spin network is the orthogonality of the dimers, namely, neighboring dimers are arranged in an orthogonal way. Another point to be mentioned is the presence of a spin frustration coming from the triangle arrangement of one J bond and two J' bonds. This frustration is introduced irrespective of the sign of J' so long as J is antiferromagnetic ($J>0$). In fact, one expects J being antiferromagnetic considering the dimer bridging angle (Cu-O-Cu) of 102.42°, since there is in general an inverse correlation between the value of J and the angle at the bridging oxygen atom, and J changes its sign near 97.6°.[10]

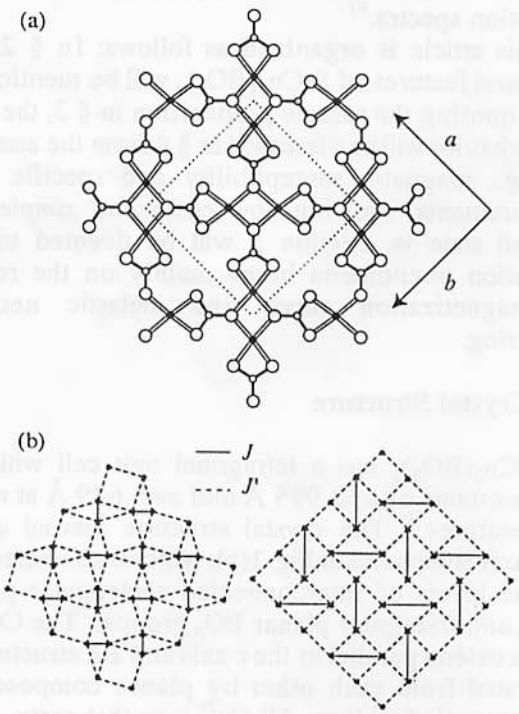

Fig. 1 (a) Crystal structure of $SrCu_2(BO_3)_2$ viewed along [001]. The closed circles, small open circles, and large open circles denote, respectively, the Cu^{2+}, B^{3+}, and O^{2-} ions. The unit cell is represented by dotted lines. (b) The real lattice of the magnetic Cu^{2+} ions in $SrCu_2(BO_3)_2$ (left) and the imaginary lattice for the Shastry-Sutherland model (right).

§3. Sample Preparation

Polycrystalline sample of $SrCu_2(BO_3)_2$ was synthesized using a conventional solid state chemical reaction. The starting materials, $SrCO_3$, CuO and B_2O_3 with high purities were weighed and intimately mixed. B_2O_3 was enriched by 5 % from the stoichiometric ratio because B_2O_3 is easy to evaporate during the following heating process. The mixed sample was ground, pelletized and slowly heated up to 850 °C in flowing oxygen gas (P_{O_2}=1 atm). The bulk single crystals, easily cleaved along the c plane, were successfully grown by a traveling solvent floating zone method using $LiBO_2$ as a flux.[11] FZ-T10000N 10 KW high-pressure type (Crystal System. Inc.) was used, which has four halogen lamps as heat sources. For the neutron scattering measurement, 99.6% ^{11}B-enriched single crystals, $SrCu_2(^{11}BO_3)_2$, were grown using $Li^{11}BO_2$ flux in order to minimize the neutron absorption by the natural abundance of ^{10}B.

§4. Exact Dimer Ground State

4.1 Magnetic susceptibility

The raw data of the parallel and perpendicular magnetic susceptibilities, $\chi_{r//}$ and $\chi_{r\perp}$, respectively, measured in a magnetic field H of 1 T are shown in Fig. 2.[5,12] It was found that the anisotropy of the susceptibilities originates only from the anisotropic

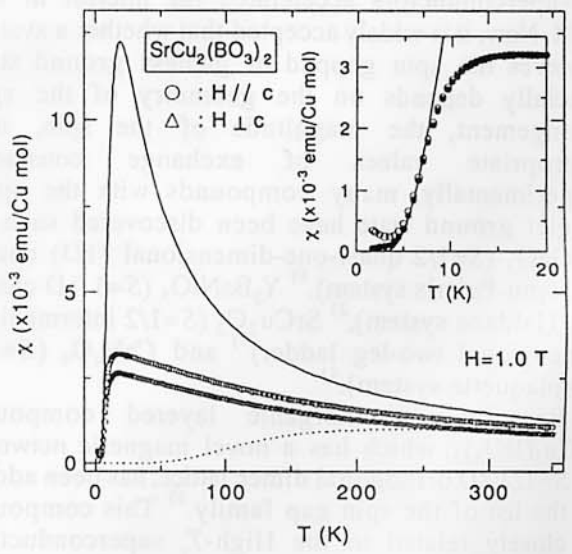

Fig. 2 Magnetic susceptibilities, $\chi_{r//}$ and $\chi_{r\perp}$, as a function of temperature in a magnetic field of 1 T applied parallel (open circles) and perpendicular (open triangles) to the c axis, respectively. The solid and broken curves are the trials to fit the experimental data to the isolated dimer model. Inset is the enlarged plot of $\chi_{r//}$ vs. T. Closed circles denote the parallel spin susceptibility. The theoretical curve is drawn by the solid line as described in the text.

g-factors: the anisotropic factor $\chi_{r//}/\chi_{r\perp}=1.10$ is just identical to that of the g-factors ($g_{//}=2.28$ and $g_{\perp}=2.07$) obtained from electron spin resonance (ESR).[13] Using the g-factors above, both data in the temperature T range of 160 K to 400 K can be fitted to the Curie-Weiss equation with $S=1/2$ and the Weiss temperature of $\theta=-102.5$ K accompanied with a temperature-independent term $\chi_0=-2.603\times10^{-5}$ emu/mol Cu. As temperature is decreased, the susceptibilities show a maximum at around 15 K and then rapidly drop toward zero with approaching $T=0$, suggesting the existence of an energy gap in the spin excitation spectrum. A small Curie like upturn is seen in the raw data below 4 K, which would appear due to magnetic impurities and/or defects of Cu^{2+} ions in $SrCu_2(BO_3)_2$. This extrinsic term was estimated by fitting the raw data below 3.5 K to C/T, where C denotes the Curie constant. The obtained value of $C=1.5\times10^{-3}$ emu K/mol Cu, corresponds to only 0.14 % of free one-half spins. As shown in the inset of Fig. 2, parallel spin susceptibility $\chi_{s//}$ was obtained by subtracting $(C/T+\chi_0)$ from $\chi_{r//}$. Finally, by the fitting $\chi_{s//}$ between 1.7 K and 7 K with $\chi_{s//}\propto\exp(-\Delta/T)$ (the solid line), the value of the spin gap Δ was evaluated to be 34 K.

4.2 Other measurements

The spin-gapped nature in this material has been also observed by Cu nuclear quadrupole resonance (NQR),[5] specific heat,[14] Cu and B nuclear magnetic resonance (NMR),[15] ESR,[13] Raman scattering,[16] magnetization curve[5, 12] and inelastic neutron scattering.[6] The obtained values of Δ are summarized in Table 1. One can see that all measurements consistently yield 34 K as the spin gap energy. Hereafter, let me pick up some results to demonstrate how Δ has been estimated in each case.

Take an example of the Cu-NQR,[5] the spin lattice relaxation T_1 was measured using the polycrystal in the temperature range between 1.5 K < T < 5 K for a center of the NQR spectra of ^{63}Cu which appears at around 23 MHz. As shown in Fig. 3, the observed spin lattice relaxation rate $1/T_1$ shows an activated type of the temperature dependence, $1/T_1\propto\exp(-\Delta/T)$, with $\Delta=30$ K.

Table. 1 Spin gap energy Δ estimated from various measurements.

method	Δ	Refs.
magnetic susceptibility	34 K	[12]
Cu NQR-T_1	30 K	[5]
Cu NMR-Knight shift	35 K	[15]
B NMR-T_1	36 K	[15]
specific heat	35 K	[16]
magnetization curve	31 K	[12]
ESR	35 K	[13]
neutron scattering	34 K	[6]
Raman scattering	34 K	[16]

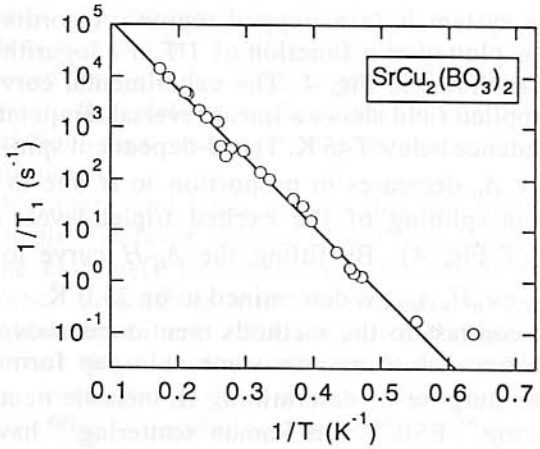

Fig. 3 Temperature dependence of $1/T_1$ at ^{63}Cu nuclear measured by the saturation recovery and inversion recovery methods on the center line of the quadrupole spectrum. The solid line shows the activated T dependence with $\Delta=30$ K.

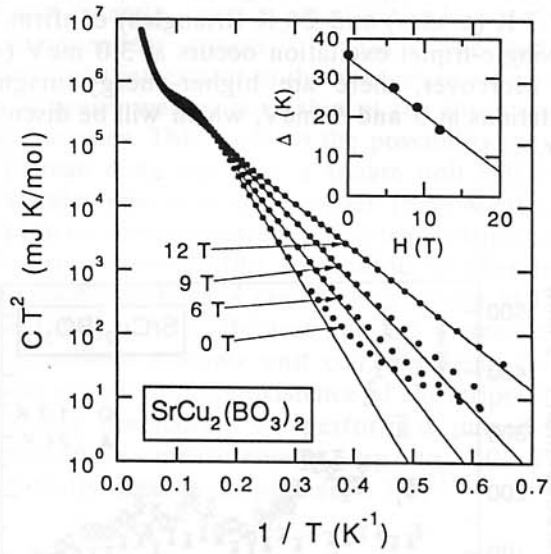

Fig. 4 Logarithmic plot of CT^2 as a function of $1/T$. Solid lines denote the calculations as described in the text. Inset shows the magnetic field variation of Δ_H.

The next example is the specific heat measurement performed by a heat-relaxation method in magnetic fields up to 12 T in a temperature range between 1.3 K and 25 K.[14] A bulk single crystal of $SrCu_2(BO_3)_2$ was used for the measurement. Because of absence of the appropriate theory to describe this experiment for the whole T region, the obtained data were analyzed only in the low-T region using an isolated dimer model in which the magnetic specific heat C_H for $T\rightarrow0$ can be expressed as $C_H\propto T^{-2}\exp(-\Delta/T)$ so long

as the system is in a gapped region. Accordingly, $C_H T^2$ is plotted as a function of $1/T$ in a logarithmic scale as shown in Fig. 4. The experimental curve at any applied field shows a linear reversal temperature dependence below T<5 K. The H-dependent spin-gap energy Δ_H decreases in proportion to H due to the Zeeman splitting of the excited triplet levels (the inset of Fig. 4). By fitting the Δ_H-H curve to $\Delta_H = \Delta_{H=0} - g\mu_B H$, $\Delta_{H=0}$ is determined to be 35.0 K.

In contrast to the methods mentioned above, in which one has to assume some spin-gap formulas for the purpose of determining Δ, inelastic neutron scattering,[6] ESR[13] and Raman scattering[16] have a great advantage in ability that the direct observation of the transition from the spin-singlet ground state to the low-lying excited triplet state is possible. The inelastic neutron scattering was curried out at the Japan Research Reactor 3M in Japan Atomic Energy research Institute, Tokai Establishment. As shown in Fig. 5, the energy scans at Q=(2, 0, 0) measured at T=1.7 K (circles) and 24 K (triangles) confirm that the single-triplet excitation occurs at 3.0 meV (=34 K). Moreover, there are higher-energy magnetic excitations at 5 and 9 meV, which will be discussed later.

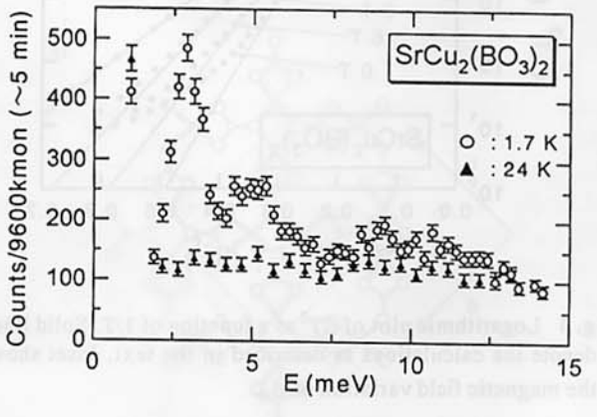

Fig. 5 Inelastic neutron scattering data: energy scans at Q=(2, 0, 0) obtained at T=1.7 K (circles) and 24 K (triangles).

4.2 Shastry-Sutherland model

Having confirmed the existence of the spin gap with Δ=34 K, the next step is to demonstrate in what way the system achieves the spin-singlet ground state. The most striking feature with respect to its ground state of $SrCu_2(BO_3)_2$ is that this material is the correspondence of the model treated by Shastry and Sutherland nearly twenty years ago.[6] They considered the lattice shown in the right-hand of Fig. 1(b) and proved that the direct product of the spin-singlet pairs is an exact ground state. If J'=0, this is evident but trivial. However, even when J' is finite, the exactness is still valid owing to the cancellation of the interdimer interactions.

Theoretically, many models have been proposed, which have the exact dimer ground state.[17] Among them, probably most famous is the Majumdar-Ghosh model for a zigzag chain with a 2 : 1 ratio of nearest and next nearest neighbor exchange constants.[18] However, there had been no examples to realize the exact models for a long time. I would like to put great emphasize on the fact that $SrCu_2(BO_3)_2$ is the first material with the exact dimer ground state.

Let me discuss the effect of J', which brings the spin frustration into the system, on the T dependence of the magnetic susceptibility. If one neglects J' (=0), the system is reduced to an S=1/2 isolated dimer model that is simplest among spin-gap systems and widely known to be applicable to many materials such as various Cu complexes.[19] Although $\chi_{//}$ was fitted to the simplest model (the solid curve) in such a way that the temperature at maximum $\chi_{//}$ (=15 K) coincides with that of the model, there is quite a large deviation as seen in Fig. 2. If one tries to fit in high-temperature region, the theoretical curve (the broken curve) begins to deviate at 250 K, yielding too large value of Δ. The big inconsistency with the isolated dimer model was also observed in the specific heat above 5 K.[14] These facts indicate that J' can not be neglible at all: the dimers should be strongly correlated within each layer and thus the system is highly frustrated. Actually, Miyahara and Ueda expressed θ and Δ as a function of J and J'. Using the experimental values θ=-92.5 K and Δ=30 K (earlier data for the powdered sample),[5] J=100 K and J'=68 K were determined.[7] Later, this set of the exchange constants is corrected to J=110 K and J'=75 K,[20] using θ=-102.5 K and Δ=34 K.[12] Moreover, their calculation with J=100 K and J'=68

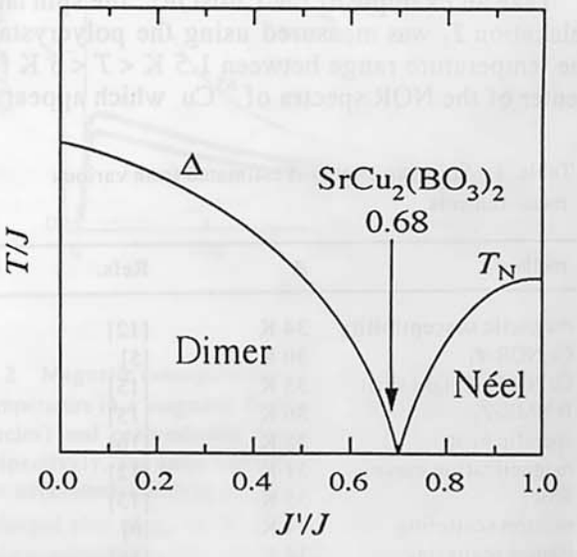

Fig. 6: Schematic phase diagram for the Shastry-Sutherland model.

K successfully reproduced our χ-T data.[7]

The phase diagram for the Shastry-Sutherland model was also proposed by Miyahara and Ueda as schematically shown in Fig. 6.[7] They showed that, as J'/J is increased, a first order phase transition to a Néel ordered state occurs at the critical boundary $(J'/J)_c$=0.70 (0.69[21]). The existence of the Néel state above $(J'/J)_c$ would be intuitively understood if one considers the case J=0 since the lattice is reduced to a simple square lattice. Interestingly, J'/J=0.68 in $SrCu_2(BO_3)_2$ is very close to $(J'/J)_c$. It might be possible to induce the phase transition to the Néel state by, for example, applying chemical pressure though all the attempts have been unsuccessful so far.[22]

§5. Localized Triplet Excitations

5.1 Quantized magnetization plateaux

Shown in Fig. 7 are the pulsed-field magnetization curves at 1.5 K up to 42 T for the single crystal ($H \perp c$) and for the field-oriented polycrystal ($H \parallel c$).[5, 12] There is no hysteresis between the field increase and decrease processes. As in the case of the magnetic susceptibility, the difference between the parallel and perpendicular magnetizations is attributed to the anisotropic g-factors. As H is increased, the low-lying triplet excited state crosses the spin-singlet ground state at about 20 T. Subsequently, the magnetization begins to increase, but $SrCu_2(BO_3)_2$ shows a stepwise behavior in striking contrast to the classical spin system, in which the magnetization increases monotonously: two plateaux appears at 1/8 and 1/4 of the Cu full moment. By extrapolation, the phase boundary for the 1/8 plateau was determined to be 30.1-31.7 T and 26.7-28.6 T for $H \perp c$ and $H \parallel c$, respectively, and that for the 1/4 plateau 39.1-41.6 T and 35.0-39.0 T. With increasing H, we have the gapped and gapless ground states by turns: In the plateau regions, $SrCu_2(BO_3)_2$ has finite energy gaps between the ground and the lowest exited states, while, between the plateau regions, the system has no excitation gaps and the magnetization increases continuously.

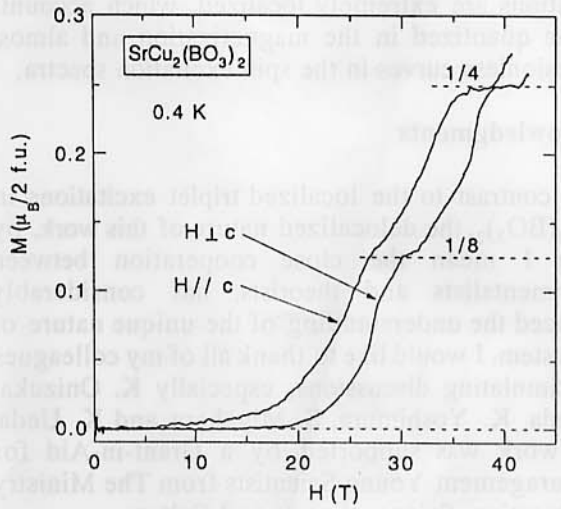

Fig. 7 Magnetization curves at 0.4 K measured perpendicular and parallel to the c axis for the single crystal and for the field-oriented polycrystal, respectively.

Miyahara and Ueda argued that the reason for the triplets to favor ordered rather than liquid states is the extremely localized character of the excited triplets:[7] originating from the orthogonality of the neighboring dimers, a hopping of the single triplet from one site to another within each plane is possible only from the sixth order in the perturbation calculations. Considering the tetragonal symmetry of the chemical structure, the necessary condition for the triplets to assure ordered structures is that corresponding magnetic unit cells are square, which is fulfilled for the 1/8 and 1/4 plateaux as shown Figs. 8(a) and 1(b), respectively. This assumption leads to other plateaux at 1/2, 1/10, 1/16, 1/32 with tetragonal symmetry.

Quite recently, more sophisticated calculation by two independent groups[23, 24] has shown that the triplet-triplet interaction at the next nearest neighbor sites is much weaker than that at the third nearest neighbor sites. This leads to the possibility that the 1/4 plateau does not have a square unit cell but a rectangular one with stripe order (Fig. 8(c)) since there are no third nearest neighbor triplet-triplet pairs in the stripe superstructure. In addition, another stripe-type superstructure was predicted to appear at 1/3 as shown in Fig. 8(d). Because the 1/3 plateau never accommodates a square unit cell, observing the 1/3 plateau is verifying the existence of the stripe order. After this prediction, we performed pulsed-field magnetization measurements up to 60 T to successfully observe the plateau at 1/3.[25]

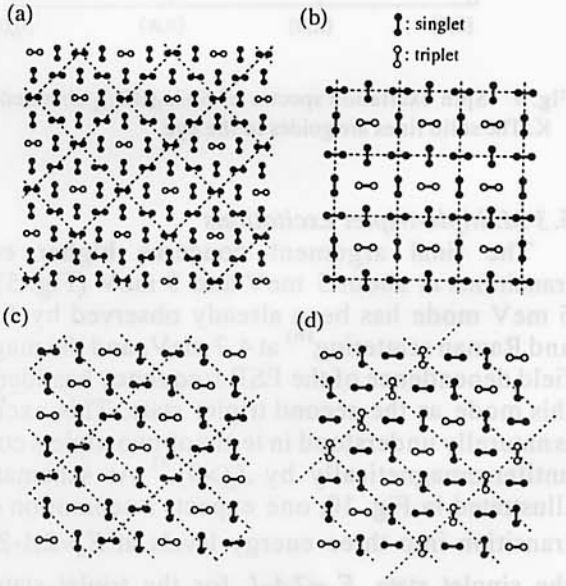

Fig. 8 Candidates of the superstructures between the excited triplets (open) and the remaining singlets (solid) for (a) the 1/8, (b), (c) the 1/4 and (d) the 1/3 plateaux.

5.2 Extremely localized single-triplet excitations

Other pieces of evidence for the localized triplet excitations have been observed by ESR,[13] NMR[15] and inelastic neutron scattering.[8] Especially, the result of the inelastic neutron scattering is important because of the direct proof of the almost localized nature of the *single*-triplet excitations. The dispersion relation of the 3 meV mode shown in Fig. 9 indicates that the excitation energies are almost Q independent. The bandwidth ΔE of 0.2 meV is significantly small in contrast to conventional low-dimensional quantum spin systems, in which strong dispersions of the single-triplet excitations were experimentally obtained, for example, ΔE=14 meV for $CuGeO_3$[26] and 7 meV for CaV_4O_9.[27] On the contrary, well-isolated clusters of exchange-coupled paramagnetic ions clearly exhibit flat dispersions in the spin excitation spectrum, for example, ΔE=0.7 meV for the isolated dimer systems $BaCuSi_2O_6$.[28] In the case of $SrCu_2(BO_3)_2$, the dimers within each plane are strongly interacting and moreover the system is located in the vicinity of the Néel ordered state so that the orthogonality of the dimers no doubt leads to the almost flat dispersion in the present spin system.

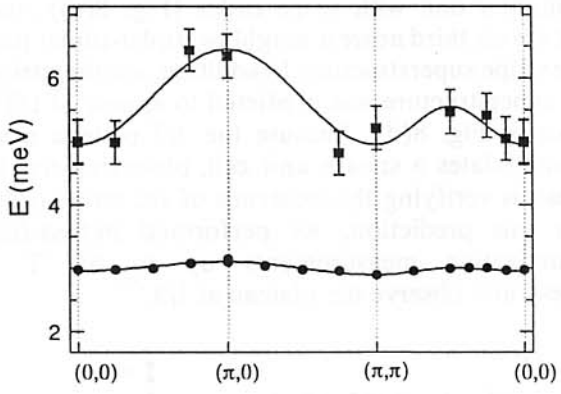

Fig. 9 Spin excitation spectra of $SrCu_2(BO_3)_2$ obtained at 1.7 K. The solid lines are guides to the eye.

5.3 Multiple-triplet excitations

The final argument concerns higher energy transitions at about 5 meV and 9 meV (Fig. 5). The 5 meV mode has been already observed by ESR.[13] and Raman scattering[16] at 4.7 meV, and the magnetic field dependence of the ESR frequency has identified this mode as the second triplet state. This excitation is naturally understood in terms of two triplets coupled antiferromagnetically by $J_t(>0)$.[8] As schematically illustrated in Fig. 10, one expects a separation of the transition into three energy levels at $E_0=2\Delta-2J_t$ for the singlet state, $E_1=2\Delta-J_t$ for the triplet state, and $E_2=2\Delta+J_t$ for the quintet state. Using E_1=4.7 meV[13,16] and E_0=3.7 meV,[16] J_t is estimated to be 1.1-1.3 meV. Similarly, the 9 meV mode would come from correlated three-triplet excitations or more though rather small peak intensity as well as broad line width does not allow a reliable discussion of this mode.

Shown in Fig. 9 is the Q dependence of the 5 meV mode. The bandwidth of ΔE=1.5 meV is once again very narrow compared with conventional low-dimensional spin gap systems, indicating the localized nature of the two-triplet excitations. However, I would like to stress the fact that this width is much wider than 0.2 meV for the single-triplet mode. This indicates that the propagation of correlated two triplets is much easier than that of the single triplet. This observation is theoretical supported by the preliminary consideration by Miyahara and Ueda that two triplets sitting on the nearest neighbor sites can propagate within the fourth-order perturbation calculations.[20]

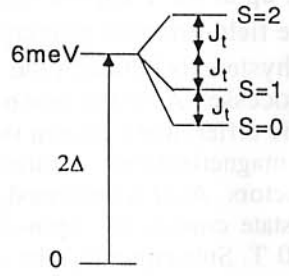

Fig. 10 Schematic energy diagram of the two-triplet excitation.

§7. Summary

We have established that $SrCu_2(BO_3)_2$ is a highly frustrated 2D spin gap system with Δ=34 K and with the exactly solvable ground state, realizing the Shastry-Sutherland model. Moreover, originating from the orthogonal network of the dimers, the triplet excitations are extremely localized, which accounts for the quantized in the magnetization and almost dispersionless curves in the spin excitation spectra.

Acknowledgments

In contrast to the localized triplet excitations in $SrCu_2(BO_3)_2$, the delocalized nature of this work, by which I mean the close cooperation between experimentalists and theorists, has considerably advanced the understanding of the unique nature of this system. I would like to thank all of my colleagues for stimulating discussions, especially K. Onizuka, Y. Ueda, K. Yoshimura, S. Miyahara and K. Ueda. This work was supported by a Grant-in-Aid for Encouragement Young Scientists from The Ministry of Education, Science, Sports and Culture.

1) M. Hase, I. Terasaki and K. Uchinokura: Phys. Rev. Lett.

70 (1993) 3651.
2) J. Darriet and J. P. Regnault: Solid State Commun. **86** (1993) 409.
3) M. Azuma, Z. Hiroi, M. Takano, K. Ishida and Y. Kitaoka: Phys. Rev. Lett. **73** (1994) 2626.
4) S. Taniguchi, T. Nishikawa, Y. Yasui, Y. Kobayashi, M. Sato, T. Nishioka, M. Kontani and K. Sano: J. Phys. Soc. Jpn. **64** (1995) 2758.
5) H. Kageyama, K. Yoshimura, R. Stern, N. V. Mushnikov, K. Onizuda, M. Kato, K. Kosuge, C. P. Slichter, T. Goto and Y. Ueda: Phys. Rev. Lett. **82** (1999) 3168.
6) B. S. Shastry and B. Sutherland: Physica **108** B (1981) 1069.
7) S. Miyahara and K. Ueda: Phys. Rev. Lett. **82** (1999) 3701.
8) H. Kageyama, M. Nishi, N. Aso, K. Onizuka, T. Yosihama, K. Nukui, K. Kakurai, K. Kodama and Y. Ueda: to appear in Phys. Rev. Lett.
9) R. W. Smith and D. A. Keszler: J. Solid State Chem. **93** (1991) 430.
10) V. H. Crawford, H. W. Richardson, J. R. Wasson, D. J. Hodgson and W. E. Hatfield: Inorg. Chem. **15** (1976) 2107.
11) H. Kageyama, K. Onizuka, T. Yamauchi and Y. Ueda: J. Crystal Growth **206** (1999) 65.
12) H. Kageyama, K. Onizuka, T. Yamauchi, Y. Ueda, S. Hane, H. Mitamura, T. Goto, K. Yoshimura and K. Kosuge: J. Phys. Soc. Jpn. **68** (1999) 1821.
13) H. Nojiri, H. Kageyama, K. Onizuka, Y. Ueda and M. Motokawa: J. Phys. Soc. Jpn. **68** (1999) 2906.
14) H. Kageyama, H. Suzuki, M. Nohara, K. Onizuka, H. Takagi and Y. Ueda: Physica B **281** & **282** (2000) 667.
15) K. Kodama *et al.*: unpublished.
16) P. Lemmens, M. Grove, M. Fisher, G. Güntherodt , H. Kageyama, K. Onizuka and Y. Ueda: Physica B **281** & **282** (2000) 656.
17) See, for example, T. Oguchi and H. Kitatani: J. Phys. Soc. Jpn. **64** (1994) 612. and the references therein.
18) C. K. Majumdar and D. K. Ghosh, J. Math. Phys. **10** (1969) 1399.
19) D.J. Hodgson: Prog. Inorg. Chem. **19** (1975) 173.
20) S. Miyahara and K. Ueda: private communication.
21) Z. Weihong, C. J. Hamer and J. Oitmaa: Phys. Rev. B **60** (1999) 6608.
22) K. Kageyama, K. Onizuka, Y. Ueda, S. Hane, H. Mitamura, T. Goto, K. Yoshimura and K. Kosuge: *Proc. 4th Int. Symp. Advanced Physical Fields, ed. G. Kido (National Research Institute for Metals, Tsukuba, Japan, 1999) p. 235-237.*
23) S. Miyahara and K. Ueda: Phys. Rev. B **61** (2000) 3417.
24) T. Momoi and K. Totsuka: Phys. Rev. B **61** (2000) 3231.
25) K. Onizuka, H. Kageyama, Y. Narumi, K. Kindo, Y. Ueda and T. Goto: J. Phys. Soc. Jpn. **69** (2000) 1016.
26) M. Nishi, O. Fujita and J. Akimitsu: Phys. Rev. B **50** (1994) 6508.
27) K. Kodama, H. Harashina, H. Sasaki, Y. Kobayashi, M. Kasai, S. Taniguchi, Y. Yasui, M. Sato, K. Kakurai, T. Mori and N. Nishi: J. Phys. Soc. Jpn. **66** (1997) 793.
28) Y. Sasago, K. Uchinokura, A. Zheludev and G. Shirane: Phys. Rev. B **55** (1997) 8357.